Atomic and electronic structure of β-SiC(001)-(3×2)

Wenchang Lu, Peter Krüger, and Johannes Pollmann
Institut für Theoretische Physik II-Festkörperphysik, Universität Münster, Wilhelm-Klemm-Straße 10, D-48149 Münster, Germany
(Received 15 October 1998; revised manuscript received 12 February 1999)

A reconstruction model for the cubic SiC(001)-(3×2) surface, which we call two adlayer asymmetric-dimer model (TAADM), is suggested on the basis of *ab initio* pseudopotential total energy and grand canonical potential calculations. Within this model, *two* Si adlayers with a nominal total coverage of one monolayer are adsorbed on the clean Si-terminated surface. Asymmetric dimers are formed in the top adlayer with a dimer-bond length of 2.24 Å. This reconstruction model overcomes all shortcomings of previous models, such as the single-dimer-row, alternate-dimer-row, and double-dimer-row models, and it is the most stable structure among all configurations which we have considered. The calculated surface-band structure, as well as the filled- and empty-state scanning tunneling microscope images for our TAADM, are in very good agreement with experimental observations. [S0163-1829(99)11227-X]

I. INTRODUCTION

The polar β-SiC(001) surface has attracted much attention both in experiment[1] and theory[2] because of its fundamental interest and technological importance. In experiment, a number of reconstructions has been observed by low-energy electron diffraction (LEED),[3,4] Auger electron spectroscopy (AES),[3–5] soft x-ray photoemission spectroscopy (XPS),[6,7] and scanning tunneling microscopy (STM).[8–11] Many *ab initio* and empirical calculations have been carried out for (2×1),[12–16] $c(4\times2)$,[17–19] and (3×2) (Refs. 14 and 20) structures. In the present paper, we focus on the (3×2) reconstruction.

The (3×2) reconstruction is the most widely studied member of the ($n\times2$) family for the Si-rich β-SiC(001) surface. It was confirmed that this reconstruction is formed by adsorption of additional Si atoms on the Si-terminated surface. Hara *et al.*,[4] using medium-energy ion scattering (MEIS), have shown that the Si coverage decreases in the order $(3\times2)>(5\times2)>(7\times2)>c(4\times2)\approx(2\times1)$. In order to explain the (3×2) reconstruction, Dayan[3] first proposed a double-dimer-row model (DDRM) in which the Si adlayer atoms form dimer rows with every third dimer row missing. This model leads to a Si adatom coverage of $\Theta=2/3$. Kaplan[5] applied this model to explain his experimental results and found that the asymmetric dimers may account for the streaking in the LEED pattern along the $[\bar{1}10]$ direction. He also pointed out that the ''3×'' direction in the (3×2) phase is parallel to the ''2×'' direction in the (2×1) phase. Hara *et al.*[8] adopted the DDRM to explain their STM images and arrived at a structure which exhibits an inter-dimer buckling. Molecular-dynamics simulations by Kitabatake and Greene,[20] employing an empirical Si potential as suggested by Tersoff,[21] arrived at the result that the DDRM has the lowest energy. Yeom *et al.*[22] have studied the (3×2) surface using high-resolution core-level photoemission. Three different Si $2p$ surface components have been identified with binding-energy shifts of -0.58, -0.92, and -1.27 eV. The DDRM was adopted by these authors to explain their results qualitatively. We will show later that the DDRM cannot explain the observed core-level shifts.

A (3×2) reconstruction pattern can also be explained by a Si adatom coverage $\Theta=1/3$. Similar to the DDRM, a single-dimer-row model (SDRM) was proposed by Hara *et al.*[4] However, this model failed to explain the STM images discussed by the same authors in a later publication[8] and by Semond *et al.*[9] On the basis of *ab initio* calculations, Yan, Smith, and Jónsson[14] proposed a different model, the alternate-dimer-row model (ADRM), for the coverage $\Theta=1/3$. In their results, the ADRM turns out to be energetically more favorable than the SDRM. We note already at this point that our calculations yield a significantly different conclusion for the relative stability of these two models (see Sec. III). The ADRM was adopted by Semond *et al.*[9] to explain their STM images and height profiles. Their results seem to support the ADRM in which the asymmetric dimers are oriented along the 3× direction and are tilted in the very same direction. This is, however, in conflict with the LEED data.[5] The 3× direction in the ADRM should be perpendicular to the 2× direction in the (2×1) surface, while the LEED pattern shows it to be parallel to the latter direction.

Here we report results of an extensive study of structural and electronic properties of the (3×2)-reconstructed SiC(001) surface. The results of our calculations show that a structural model with a coverage of $\Theta=1$ is energetically most favorable. In this structure, however, the adatoms do not form a complete monolayer but they are rather distributed within two adlayers, as discussed below. Our calculated optimal configuration is in gratifying agreement with a whole body of recent experimental data.

In Sec. II, the calculational method is briefly outlined. In Secs. III, IV, and V, we discuss various investigated models with $\Theta=1/3$, 2/3, and 1, respectively. The grand canonical potential for models with these different coverages is compared in Sec. VI and an assessment of the most stable configuration is made. A summary concludes the paper in Sec. VII.

II. CALCULATIONAL METHOD

Ab initio pseudopotential calculations have been carried out within local-density approximation[23] (LDA) of density-

TABLE I. Decay constants (in atomic units) used in our calculations.

Atom	Decay constants
Surface Si atoms	0.18, 0.5, 1.0
Bulk Si atoms	0.2, 0.6
Bulk C atoms	0.35, 1.7
Saturating H atoms	0.35

functional theory (DFT). Nonlocal, norm-conserving pseudopotentials in separable form, as suggested by Kleinman and Bylander,[24] and the exchange-correlation functional of Ceperley and Alder,[25] as parametrized by Perdew and Zunger,[26] are employed in our calculations. For the carbon atoms, a very smooth pseudopotential is used to reduce the numerical effort.[12] The supercell technique with six atomic layers and six vacuum layers is used to describe the surface system. For one of the models considered, the most stable TAADM, we have also calculated, with a supercell including ten atomic layers and eight vacuum layers, the results on the structure parameters, as well as surface bands which are very similar to those with the supercell including six atomic layers and six vacuum layers. The dangling bonds at the bottom of the slabs in each supercell are saturated by hydrogen atoms to avoid artificial electronic states originating from the ideal surface within the fundamental gap. The wave functions are expanded in terms of linear combinations of Gaussian orbitals with s, p, d, and s^* symmetry. For the s,p,d symmetry, the Gaussian orbitals are defined as

$$\varphi_{lm}(\mathbf{r}) = N_{lm} Y_{lm}(\theta,\phi) r^l e^{-\alpha r^2}, \quad l=0,1,2, \quad m=-l,\ldots,l, \tag{1}$$

where Y_{lm} are the spherical harmonics and N_{lm} are the normalized factors. For the s^* symmetry, the Gaussian orbital is defined as

$$\varphi_{s^*}(\mathbf{r}) = N_{s^*} r^2 e^{-\alpha r^2}. \tag{2}$$

These ten orbitals form one shell with the decay constant α. Two decay constants, i.e., 20 orbitals per atom, are used for the bulk Si and C atoms. In order to take the spatial extent of the wave functions into vacuum better into account, three decay constants, i.e., 30 orbitals per atom, are used for the substrate-surface Si atoms and Si adatoms. One decay constant, i.e., 10 orbitals per atom, is used for the saturating H atoms. The decay constants are listed in Table I. In order to check if the above basis set is accurate enough, we have computed the total-energy difference between the various structural models by using larger basis sets (up to 40 Gaussian orbitals per atom). It is found that the error in total energy difference is less than 0.1 eV per (3×2) unit cell. By comparing this error with the large formation energy difference (see Sec. VI), we can safely conclude that the above basis set is accurate enough for the present investigation.

Integrals over the Brillouin zone are performed using the special $\mathbf{k}_\parallel$-point approach. For the (3×2) unit cell, 16 $\mathbf{k}_\parallel$ points in the surface Brillouin zone turn out to be sufficient for good convergence. To obtain the most stable geometric structure, all atoms in the adsorbed Si layers and in the first three SiC substrate-surface layers are relaxed to eliminate the forces. The structure optimization is stopped when each force is less than 10^{-3} Ry/a.u. The modified Broyden scheme is used in this optimization.

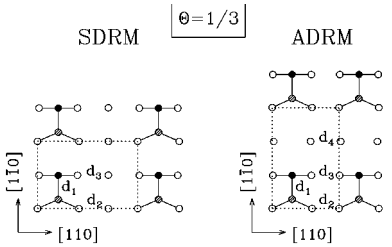

FIG. 1. Top views of the optimized structures for the (3×2) SDRM (left panel) and the (2×3) ADRM (right panel). Open circles represent Si substrate-surface layer atoms, solid and shaded circles represent up and down atoms in the adatom dimers, respectively. The (3×2) and (2×3) unit cells are indicated by dashed lines.

STM images are calculated in the framework of the Tersoff-Hamann approach.[27] A plane at 1.5 Å above the topmost adatoms is selected to represent the charge density which simulates the STM image. We have also calculated the image with a plane at 2.5 Å above the topmost adatoms. There is no significant difference between both STM images. Our calculations show that the voltage plays only a minor role in the interpretation of filled- or empty-state STM images for the systems with asymmetric dimers in the top layer. For example, when the voltage changes from 0.5–2.5 eV, we did not find any significant change in the images. We also find that the highest occupied surface state and the lowest empty surface state dominate the filled- and empty-state images, respectively. In the following therefore the STM images are simulated with the charge density of a plane at 1.5 Å above the topmost adatoms and the voltage is chosen such that only the highest occupied or the lowest unoccupied surface state is included.

III. SI COVERAGE $\Theta = 1/3$

In this section we address models which are based on the assumption that a low coverage of Si atoms is responsible for the observed (3×2) reconstruction of the SiC(001) surface. We label the case of 1/3 monolayers (ML) of Si adatoms adsorbed on the Si-terminated β-SiC(001) surface as $\Theta = 1/3$. Top views of the optimized structures as resulting from our calculations for two different reconstruction models with $\Theta = 1/3$ are shown in Fig. 1. One of these structures corresponds to the SDRM (left panel of Fig. 1), as proposed by Hara *et al.*,[4] which is also called added dimer-row model.[1] In this model, the adlayer contains one row of Si adatoms for every three possible rows of bulk spacings along the $\times2$ direction (see left panel of Fig. 1). The other is the ADRM (right panel of Fig. 1), which was first proposed by Yan, Smith, and Jónsson[14] on the basis of their *ab initio* calculations and was used by Semond *et al.*[9] to explain their STM data. In this model, the dimers in the adlayer are arranged in an alternate way to form a (2×3) reconstruction (i.e., the unit cell is merely turned around by 90° with respect to the SDRM) and the dimer direction is now parallel to the $\times3$ direction (see right panel of Fig. 1).

TABLE II. Bond lengths (in Å) for the single-dimer-row model (SDRM) and alternate-dimer-row model (ADRM). The structure parameters are defined in Fig. 1. Δz, which is not indicated in Fig. 1, is the height difference between up and down atoms in the asymmetric dimers.

Structure	d_1	d_2	d_3	d_4	Δz
SDRM: present work	2.28	2.70	2.84		0.54
SDRM: Yan *et al.* (Ref. 14)	2.65	2.43	2.43		0.00
ADRM: present work	2.26	2.48	2.60	2.77	0.52
ADRM: Yan *et al.* (Ref. 14)	2.28	2.60	2.75	2.29	0.52

The geometric structure for both the SDRM and the ADRM is optimized by relaxing all atoms in the adlayer and those in the topmost three substrate-surface layers. Our calculations show that the dimers in the adlayer are highly asymmetric for both models. The structure parameters for the optimized configurations are listed in Table II. The dimer-bond length of 2.28 Å in the SDRM is characteristic for the Si-Si bulk-bond length. The dimer-tilt height of 0.54 Å between up and down atoms in the asymmetric dimers results in a buckling angle of 13.7°. The distances between neighboring substrate-surface Si atoms $d_2=2.70$ Å and $d_3=2.84$ Å are in the order of the surface-layer bond length at the clean Si-terminated SiC(001) surface.[2] In the ADRM, the dimer-bond length of 2.26 Å, the dimer-tilt angle of 13.2° and the dimer-tilt height of 0.52 Å are very similar to those in the SDRM. The distances d_2 and d_3 decrease due to the adsorption of Si atoms. Finally, d_4 is very close to the distance between neighboring Si surface-layer atoms at the clean SiC(001)-(2×1) surface[12] since the two atoms do not bond to any adatom. The above results indicate that the dimerization of the adatoms in both models is very similar. The only difference is the lateral *arrangement* of the dimers.

The structure parameters obtained by Yan, Smith, and Jónsson[14] are also listed in Table II. There are many significant differences between the results of those authors and of our present calculations. First, for the SDRM symmetric dimerization was found to be energetically more favorable than asymmetric dimerization in Ref. 14. Their dimer-bond length of 2.65 Å is much larger than the one resulting from our calculations. Nevertheless, the distance between neighboring substrate-surface Si atoms is only 2.43 Å which is even smaller than the dimer-bond length in their adlayer. Second, for the ADRM an asymmetric dimer is found in both calculations, but in the results of Yan, Smith, and Jónsson[14] the distance d_4 is much smaller (2.29 Å) than in our results (2.77 Å). In the case of the (2×1) reconstruction of the clean Si-terminated SiC(001) surface, the dimer-bond length of 2.26 Å reported in their publication is significantly different from respective values reported from other *ab initio* calculations.[12,13] This deviation is due to different $\mathbf{k}_\parallel$-point samplings employed by the different authors. While Yan, Smith, and Jónsson[14] used only one $\mathbf{k}_\parallel$ point of the surface Brillouin zone, which has been shown[12] to be insufficient for good convergence, we have used 16 $\mathbf{k}_\parallel$ points of the surface Brillouin zone. The same reason may account for the differences between their optimized configuration of the 3×2 surface and ours.

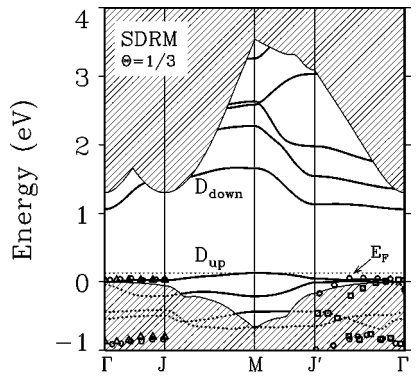

FIG. 2. Section of electronic surface-band structure of the SDRM. The projected band structure of the bulk crystal is shown by the shaded areas. The squares, triangles, and circles represent experimental ARPES data of Lindner *et al.* (Refs. 28 and 29) and of Yeom *et al.* (Ref. 30), respectively. The experimental bands have been aligned with the calculated D_{up} state at Γ to ease the comparison between theory and the different experiments.

Our calculations show that there is only a slight difference in the total energies of these two models with the SDRM being 68 meV per 3×2 unit cell *lower* than the ADRM. This is in conflict with the results obtained by Yan, Smith, and Jónsson.[14] They find the ADRM to be much more favorable than the SDRM with a large difference in total energy [3.58 eV per (3×2) unit cell]. This large deviation results mainly from the different optimized structures obtained in the two calculations.

Semond *et al.*[9] have adopted the ADRM to explain their measured height profile of empty-state STM data along the $\times3$ direction. To be in accord with the experimental observations, the following conditions for the (2×3) reconstruction should be satisfied by an appropriate structural model. First, the dimer direction should be parallel to the $\times3$ direction. Second, the dimers should be asymmetric and all dimers should be tilted in the same direction. The ADRM satisfies the above mentioned conditions, but is in conflict with LEED data[5] and the results of other experiments.[3] On the one hand, the $\times3$ direction of the (2×3) ADRM is perpendicular to the $2\times$ direction of the (2×1) reconstruction [which is formed after annealing the (2×3) surface] although these two directions should be parallel according to the LEED data for a single domain surface[5]. On the other hand, Dayan[3] has found that adsorption of hydrogen or oxygen on the (2×3) surface will result in a (1×3) reconstruction. The ADRM is in conflict with these observations, as well, since the surface will keep the (2×3) reconstruction after breaking the dimer bond in the adlayer due to adsorbates.

Now we address the electronic properties of the low-coverage case $\Theta=1/3$. Since the ADRM can be excluded on the basis of experimental results[3,5] and since it is energetically less favorable than the SDRM in the results of our calculations, we only discuss the band structure of the SDRM at this point. A section of the surface-band structure of the SDRM of SiC(001)-(3×2) is shown in Fig. 2. The projected band structure of the bulk crystal is shown by the shaded areas. In the projected band gap, there are several surface-state bands. The highest occupied surface state D_{up} and the lowest empty surface state D_{down} are mainly local-

ized at the up and down atoms of the dimers in the adlayer, respectively. The other states in the gap mainly result from an interaction of the substrate-surface Si orbitals with Si adatom orbitals. There is no overlap in energy between the D_{up} and D_{down} bands. Therefore the (3×2) surface of the SDRM is semiconducting with a band gap of roughly 1 eV. The occurrence of such a large band gap is related to the strong asymmetry of the dimers as we have pointed out in our previous work on the missing-row asymmetric-dimer model of the SiC(001)-$c(4\times2)$ surface.[19] Since there is only one dimer per (3×2) unit cell, the distances between neighboring dimers are 9.21 Å in the $3\times$ and 6.14 Å in the $\times2$ direction. These large distances give rise to a relatively weak dispersion of the surface-state bands D_{up} and D_{down}, only. The small dispersion of these bands is the second reason for the large gap. The third reason is, of course, the large bulk-band gap of cubic SiC. We remind the reader at this point that the experimental gap is considerably larger than the theoretical LDA gap, a well-known shortcoming of LDA calculations.

Experimental results for the surface-band structure as resulting from angle-resolved photoemission (ARPES) measurements are also displayed in Fig. 2 by squares,[28] triangles,[29] and circles.[30] We have aligned our calculated band structure at the Γ point with the measured band structure, i.e., with the experimental energy position of the D_{up} state at Γ. Along the Γ-J direction, the calculated surface-state band D_{up} is in agreement with experiment. The resonance band within the projected bulk-band structure near -1 eV, however, is considerably lower in energy in the experimental results than in the results of our calculations. Along the Γ-J' direction, there is some agreement between theory and experiment but there are also significant deviations between the calculated and measured bands. The measured dispersion of the D_{up} band is of the order of 0.5 eV in Ref. 29 and 0.2 eV in Ref. 30 while our calculations yield an extremely small bandwidth only. We note in passing that the band structure of the ADRM (not explicitly shown for shortness sake) shows even considerably stronger deviations from the data.

Another powerful way to confirm or disprove a certain model is to address calculated filled- and empty-state STM images in relation to experimental evidence. For example, we show in Fig. 3 calculated filled D_{up} state (top panel) and empty D_{down} state (bottom panel) STM images for the SDRM. The top view of the structure is also displayed for clarity sake (see Fig. 1 for reference). Since the surface state D_{up} is mainly localized at the up atoms which reside 0.52 Å above the down atoms, only the up atoms are visible in the filled-state image. Therefore the (3×2) reconstruction can clearly be resolved in the filled-state image. In the empty-state image, both the up and down atoms are visible since the empty D_{down} state is mainly localized at the down atoms which reside in a lower position than the up atoms. Along the $\times2$ direction, the empty-state image shows twice as many spots as the filled-state image. In experiment,[8,9] both filled- and empty-state images clearly resolve the (3×2) reconstruction. In addition, the experimental empty-state image shows two spots with different intensity along the $3\times$ direction. The SDRM fails to explain this finding since the dimer direction in the SDRM is along the $\times2$ direction.

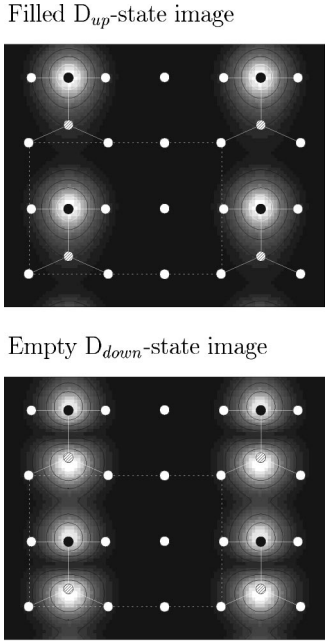

FIG. 3. Calculated filled D_{up}-state (top panel) and empty D_{down}-state (bottom panel) STM images for the SDRM. The geometry of the surface is shown by the top view (see also left panel of Fig. 1) and the rectangular unit cell is indicated by dashed lines, as well.

For the low-coverage case with $\Theta=1/3$ we can draw the following conclusions: (1) the ADRM can be excluded on the basis of the LEED (Ref. 5) and other experimental results,[3] as well as on the basis of our total-energy calculations which reveal that the ADRM is less favorable than the SDRM, (2) the (3×2) SDRM has not been observed in STM experiments, and (3) the dimer direction in the SDRM is in conflict with experimental observations in STM profiles[9]. Based on the above conclusions it seems that the case $\Theta=1/3$ does not correspond to the systems investigated in experiment, at least in the STM measurements.[9] Yoshinobu *et al.*[33] concluded from their RHEED data that they were studying back to this point.

IV. SI COVERAGE $\Theta=2/3$

Another model compatible with the (3×2) reconstruction is the double-dimer-row model (DDRM) with a Si adatom coverage of $\Theta=2/3$. For every three bulk spacings, there are two adatom rows and one missing row. This model was first proposed by Dayan[3] and later adopted by Kaplan[5] and Hara *et al.*[8] Within the DDRM there are many possibilities to arrange the dimers in the adlayer. In order to explain their measured STM images, Hara *et al.*[8] suggested a structure with *symmetric* dimers of different height, which we label as symmetric double-dimer-row model (SDDRM). As configurations with asymmetric dimers are concerned, we show top views of four different optimized structures in Fig. 4. In these structures, the asymmetric dimers are arranged in layered-antiferromagnetic (LAFM) or layered-ferromagnetic (LFM) configurations, as proposed by Kaplan,[5] or in zigzag-ferromagnetic (ZZFM) or zigzag-antiferromagnetic (ZZAFM) configurations, as considered, in addition, in the present paper. Our total-energy calculations show that the

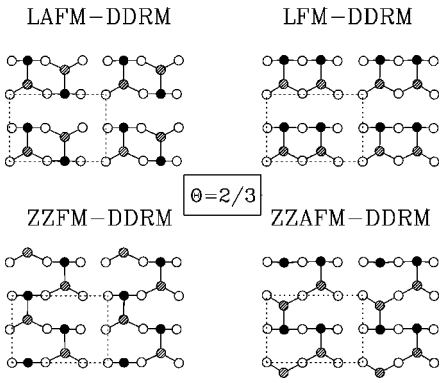

FIG. 4. Top views of the LAFM, LFM, ZZFM, and ZZAFM double-dimer-row models with $\Theta = 2/3$. The open circles represent Si substrate-surface layer atoms, the solid and shaded circles represent up and down atoms of the asymmetric dimers in the adlayer, respectively.

SDDRM is not a stable structure since its total energy is 0.9 eV *higher* than that of the models with asymmetric dimers. The total-energy differences between the LAFM, LFM, ZZFM, and ZZAFM models in Fig. 4 are less than 0.1 eV with the ZZFM configuration constituting the most stable structure. In the four configurations, the asymmetric dimers have nearly identical structural parameters. Their dimer length of about 2.3 Å, their vertical spacing between up and down atoms of about 0.5 Å, and their tilt angle of about 13° are very similar to the respective values for the asymmetric dimers in the SDRM for $\Theta = 1/3$, discussed in Sec. III, and to those which we have found for the SiC(001)-$c(4\times2)$ reconstruction.[19]

Let us now discuss the electronic structure of the most stable $\Theta = 2/3$ configuration, which is the ZZFM-DDRM (see lower left panel of Fig. 4). A section of its surface-band structure is shown in Fig. 5 together with the projected band structure (PBS) of the bulk crystal. There are two asymmetric dimers per (3×2) unit cell, not arranged in a row within the unit cell but in a staggered configuration, with the same tilts in the same direction. Their down atoms give rise to the two lowest empty surface-state bands D^1_{down} and D^2_{down} and their up atoms give rise to the two occupied surface-state bands D^1_{up} and D^2_{up}. Interestingly enough, these latter two are not the highest occupied bands, unlike the respective D_{up} band in the case of the SDRM for $\Theta = 1/3$ (see Fig. 2). In the present case of $\Theta = 2/3$, the highest occupied surface-state bands are the S_1 and the S_2 bands which originate from interacting orbitals at the Si adatoms and the Si substrate-surface layer atoms. The strong interaction between neighboring dimers within the unit cells gives rise to a strong dispersion of the S_1 band along the ΓJ and MJ' directions. These results are in conflict with recent photoemission data which show a very flat highest occupied surface-state band.[29]

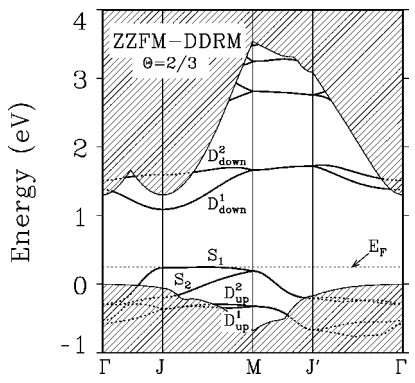

FIG. 5. Section of the surface-band structure of the ZZFM-DDRM. The projected band structure of the bulk crystal is shown by the shaded areas.

The surface-band structures of the other three DDRM's (see Fig. 4) are very similar to that of the ZZFM-DDRM except for the loss of the twofold degeneracy of the bands along the MJ' direction.

We have also calculated filled- and empty-state STM images for the four DDRM's. Since only the up atoms are visible in the filled-state images, zigzag configurations of spots are to be seen in the ZZFM-DDRM and the LAFM-DDRM. In the empty-state images, four spots per (3×2) unit cell are obtained for all the investigated DDRM's and the images seem to show (3×1) reconstructions. Such a reconstruction has never been observed in experiment. From the above analysis, we can conclude that the discussed DDRM's lack experimental support since (1) the band structure of the DDRM's is not in agreement with the ARPES data[28,29] and (2) the calculated STM images are not in accord with the available STM data.[8,9]

Yeom *et al.*[22] have used a DDRM to explain the three Si $2p$ core-level shifts which they have observed. We have calculated these core-level shifts for SiC(001)-(3×2) as total-energy differences between the ground state and the excited state with one core electron excited to be a free electron. This has been accomplished by construction of appropriate pseudopotentials according to the method of Pehlke and Scheffler.[31] A uniform background of opposite charge is added to maintain the charge neutrality. Our results for the DDRM are in conflict with the experimental observations. First, asymmetric dimers are found in our optimized configuration and the core-level shifts from the dimer up atoms are very different from those of the dimer down atoms. The former are about -0.7 eV and the latter are about $+0.1$ eV. In their paper, Yeom *et al.*[22] relate one of their observed shifts (which they labeled $S1$ and $S2$, not to be mixed up with our calculated bands S_1 or S_2) to the four adatoms in the unit cell. Second, our calculations show that the core-level shifts from all the Si substrate-surface-layer atoms are very close, and the respective value of -0.3 eV is much smaller than the shifts $S2$ (-0.92 eV) and $S3$ (-1.27 eV) observed in experiment.

In a molecular-dynamics simulation by Kitabatake and Greene,[20] it turned out that the DDRM has the lowest energy but they did not mention how the asymmetric addimers are arranged and the authors did not investigate configurations with higher Si-adatom coverage. In the next section, we discuss the case of $\Theta = 1$, and we will show that it is a very important case for the (3×2)-reconstructed SiC(001) surface.

V. SI COVERAGE $\Theta = 1$

In the present section, we consider a *model* for the (3×2) reconstruction with a Si adatom coverage of $\Theta = 1$. In the

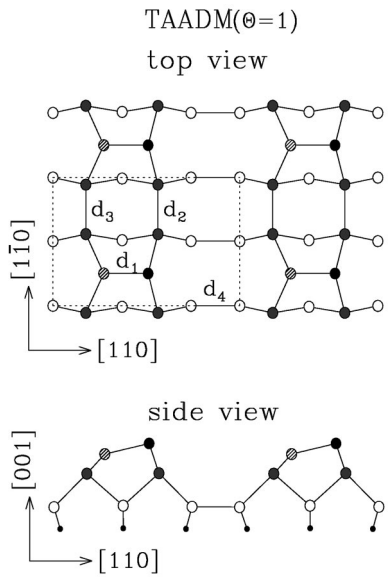

FIG. 6. Top view (top panel) and side view (bottom panel) of the TAADM with $\Theta=1$. The open circles represent Si substrate-surface layer atoms, the dotted circles indicate Si adatoms in the second adlayer and full dots, and the shaded circles indicate up and down atoms of the asymmetric dimers in the top adlayer, respectively. Bond lengths are labeled as d_i with $i=1,\ldots,4$.

optimized structure one adlayer with $\Theta=2/3$ is adsorbed on the clean Si-terminated surface, similar to the case of the DDRM, but now with symmetric dimers. An additional adlayer with $\Theta=1/3$ is adsorbed on top of the double-dimer rows of the former adlayer. We label these adlayers counted from the top of the adsorbate system the first and the second adlayer, respectively. The adatoms in the first (or top) adlayer saturate the dangling bonds of the adatoms in the second adlayer and they form asymmetric dimers. We call this model the two-adlayer asymmetric-dimer model (TAADM). A top and a side view of our optimized structure are shown in Fig. 6. In the top adlayer, the asymmetric dimer-bond length d_1 is 2.24 Å, comparable with the dimer-bond length in the top layer of the Si(001)-(2×1) surface. The height difference of 0.50 Å between the up and down atoms of these asymmetric dimers leads to a tilt angle of 12.8°. The lengths d_2 and d_3 of the symmetric dimers in the second adlayer are 2.37 and 2.38 Å and the length d_4 in the substrate-surface layer is 2.41 Å. All these bond lengths are of the order of a typical Si-Si bulk-bond length.

A section of the electronic surface-band structure is shown in Fig. 7 together with the projected band structure of the bulk crystal. The experimentally observed surface bands are also shown in the figure by squares,[28] triangles,[29] and circles.[30] The bonds in the asymmetric dimers give rise to the dimer-bond band Di, similar to the case of the Si(001)-(2×1) surface.[32] The highest occupied surface-state band, which we label D_b, results from the bonding combination of the dangling-bond states at the up and down atoms of the dimers in the top adlayer. Since the distances between neighboring dimers in the top adlayer are 9.21 Å in the $3\times$ direction and 6.14 Å in the $\times2$ direction, the dangling-bond band D_b is very flat along the Γ-J line and has a width of only 0.37 eV along the Γ-J' line. One reason for the dispersion of this band along the Γ-J' line lies in the fact that the interaction between the asymmetric dimers in the top adlayer mediated by the Si atoms in the second adlayer is strong along the $\times2$ direction. The lowest empty surface-state band, labeled D_a, which results from an antibonding combination of the dangling-bond states at the up and down atoms of the top adlayer dimers, resides near 1.1 eV and has a very weak dispersion, as well. Obviously the surface of our TAADM is semiconducting. It has an LDA band gap of 0.82 eV. The other two occupied surface-state bands S_1 and S_2 which reside in energy between the bands D_b and Di are similar to the respective S_1 and S_2 bands of the DDRM's discussed in Sec. IV. The strong dispersion of these two bands along the ΓJ direction is due to the strong interaction between the double-dimer rows in the first adlayer. The dimer-bond length of $d_4=2.41$ Å in the TAADM is much smaller than the respective value of 2.73 Å found in the case of the clean Si-terminated SiC(001)-(2×1) surface.[12]

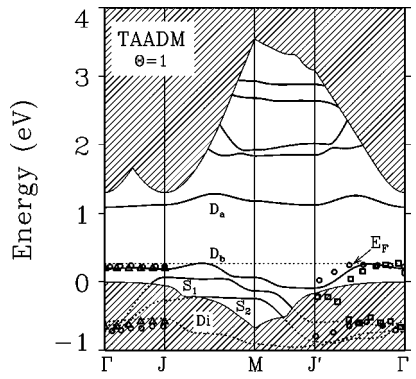

FIG. 7. Section of the surface-band structure of the TAADM. The projected band structure of the bulk crystal is shown by the shaded areas. The squares, triangles, and circles represent experimental results of Lindner *et al.* (Refs. 28 and 29) and of Yeom *et al.* (Ref. 30), respectively. The experimental bands have been aligned with the calculated D_b state at Γ to ease the comparison between theory and the different experiments.

The experimental results for the surface-band structure resulting from angle-resolved photoemission (ARPES) measurements, which we have already addressed in the context of Fig. 2, are also displayed in Fig. 7 by squares,[28] triangles,[29] and circles,[30] aligned with the measured band structure as in Fig. 2. Along the Γ-J direction, the calculated surface-state bands D_b and Di are now in good agreement with experiment. Along the Γ-J' direction, the D_b band is in very good account with the data. As to the other measured band between -0.4 and -0.8 eV, most of it is in close accord with our calculated bands. Only the relation between measured and calculated bands is somewhat more subtle. This could be related to the fact that it might be difficult to resolve the bands in this energy and $\mathbf{k}_\parallel$ region while our theoretical results clearly resolve three bands S_1, S_2, and Di. Summarizing these results of the comparison, we note that our calculated surface-state bands are in very gratifying agreement with available ARPES data.[28,29]

Calculated filled D_b- and empty D_a-state STM images of the TAADM are shown in Fig. 8. A top view of the optimized structure is also shown in the figure for convenience (see Fig. 6 for reference). We can see very clearly that the (3×2) reconstruction can be resolved in both the filled- and empty-state images. In the filled-state image, one oval spot is

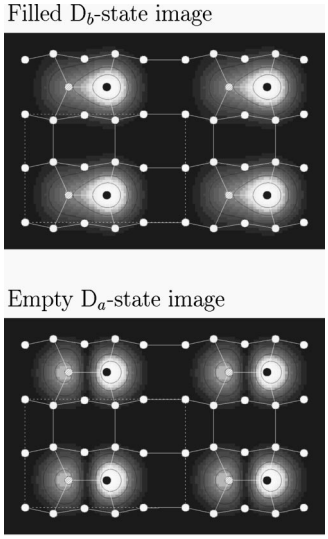

FIG. 8. Calculated filled D_b-state (top panel) and empty D_a-state (bottom panel) STM images for the TAAM. The geometry of the surface is shown by the top view (see also Fig. 6) and the rectangular unit cell is indicated by dashed lines, as well.

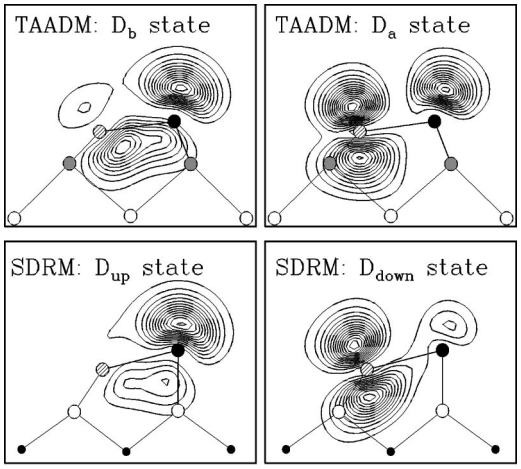

FIG. 9. Charge-density contours of the highest occupied state D_b (upper left panel), the lowest empty state D_a (upper right panel) for the TAADM, the highest occupied state D_{up} (lower left panel), and the lowest empty state D_{down} (lower right panel) for the SDRM.

observed in each (3×2) unit cell. The long axis of the oval spot is along the $3\times$ direction. The shape of the spot is different from the results for the (3×2) SDRM which we have analyzed in the case of $\Theta=1/3$ (see Sec. III for comparison), as well as, for the missing-row asymmetric-dimer (MRAD) model of the $c(4\times2)$ reconstruction,[19] although the spots originate from the asymmetric Si addimers in all these cases. First, in the present case the tilt angle of 12.8° is slightly smaller than the value of 13.7° in the other two cases. Second, the highest occupied state is not only localized at the up but also at the down atoms, a feature that differs from the respective bands in the SDRM and the MRAD model. This oval spot splits into two lobes with different intensity in the empty-state image. These results are in very good agreement with the experimental findings of Semond *et al.*[9] The two spots along the $3\times$ direction are related to the up and down atoms in the asymmetric dimers of the top adlayer. The high-intensity spot originates from the up atoms and the low-intensity spot originates from the down atoms. Since the dimer direction in the top adlayer is along the $3\times$ direction, the height profile observed in STM experiments[9] is easily intelligible.

To make the different features of the STM images of the TAADM and SDRM more transparent, we show charge-density contours of the highest occupied and lowest unoccupied surface states in Fig. 9. In the SDRM, as we have pointed out in Sec. III, the D_{up} state is mainly localized at the up atom as can clearly be seen in the lower left panel of Fig. 9. Therefore a spherical distribution is obtained for the filled-state STM image of the SDRM (see Fig. 3 for reference). Comparing the upper left with the lower left panel of Fig. 9, we observe an important difference between the SDRM and the TAADM. In the latter, the state D_b originates not only from the up atom but also from the down atom. This results in an oval distribution in the filled-state STM image of the TAADM. For the D_a state of the TAADM, two distinguishable parts localized at the up and down atoms, respectively, are observed. This feature leads to the two spots in the empty-state STM image (see Fig. 8). Since the charge density around the up atom is larger than that around the down atom, the bright spot in the STM image is from the up atom and the dark image from the down atom. This is in contrast to the SDRM in which the bright spot is from the down atom since the D_{down} state is mainly localized at the down atoms.

Since the dimer arrangement in the top adlayer of the TAADM is the same as in the ADRM which was adopted by Semond *et al.*,[9] we can explain the three observed types of defects, as well as, the ADRM. Here we use the same labels as in the literature.[9] For the ''missing-dimer defect'' (type A), the periodicity in the $\times2$ direction is not changed except for one dimer missing. For the ''dimer-pair defect'' (type B), the periodicity in $\times2$ direction shifts by one nearest-neighbor spacing. The type-C defect may be caused by different tilting directions of the asymmetric dimers or by a dimer shift along the $3\times$ direction. In the latter case, one double dimer in the second adlayer also shifts along the same direction. The feature of disorder in the empty-state image observed by Hara *et al.*[8] may be due to the fact that there are too many type-C defects in the surface. In their experiment, only one bright spot is observed per unit cell.

Yoshinobu *et al.*[33] have investigated the dependence of the surface-structure transition on the amount of the Si_2H_6 dose by RHEED. They found that the amount of the Si_2H_6 dose required for the transition of the C-terminated $c(2\times2)$ surface to the Si-rich (3×2) surface was approximately 1.36 times as large as the dose necessary to induce the $c(2\times2)$ to (2×1) transition. Based on the assumption that the (2×1) and the $c(4\times2)$ surfaces are related to the clean Si-terminated surface, there should be 1/3 monolayers of Si adatoms adsorbed on the clean surface. As we have pointed out in our previous study,[19] the $c(4\times2)$ reconstruction is stabilized by adsorption of half a monolayer of Si adatoms on top of the clean surface. We have shown as well that a (2×1) structure exists at this coverage. Taking this into account, the transition from the C-terminated $c(2\times2)$ structure to the (2×1) structure requires 1.5 monolayers of

Si, while the transition from $c(2\times2)$ to the (3×2) described by the TAADM requires 2 monolayers of Si. The ratio of 2/1.5=1.33 is in good agreement with experiment.[33]

Dayan[3] and Hara *et al.*[34] observed a phase transition from the (3×2) to a (3×1) surface by exposing the (3×2) surface to hydrogen at room temperature. An opposite phase transition from the (3×1) to the (3×2) surface occurs when the substrate temperature is raised to 1000 °C. The hydrogen-induced phase transition can occur in two different ways. If the dimers were broken by hydrogen termination, each Si atom in a dimer would be terminated by two hydrogen atoms saturating its two dangling bonds. In our TAADM, the surface keeps its (3×2) reconstruction since the dimerization is along the $3\times$ direction. This is not in accord with the experimental observation. The other way is the abstraction of Si atoms due to hydrogen, i.e., Si and H atoms form the gas phase of SiH_4 or of Si_2H_6. In this way, the amount of Si atoms at the surface is different before and after the phase transition. The reversible phase transition observed in experiment[3,8] can be understood in the following way. First, the Si adatoms in the top adlayer of the TAADM are abstracted by exposing the surface to hydrogen. The surface shows a metastable (3×2) DDRM. Second, the hydrogen atoms saturate all dangling bonds of the adatoms in the second adlayer and the dimers are broken. The surface then shows a H-induced (3×1) reconstruction. By raising the substrate temperature, the H atoms are desorbed and the surface transforms into the metastable (3×2) DDRM. The latter, as well as the (3×2) TAADM, may be indistinguishable without careful LEED-IV data. Therefore a reversible phase transition is observed. STM measurements before and after hydrogenation would be helpful to better understand this process. From our analysis, the STM images should be different before and after hydrogenation.

Our calculations of Si $2p$ core-level shifts for the TAADM give the following results. For the up atoms of the asymmetric dimers in the top adlayer the core-level shift is -0.65 eV. For the down atoms, it is only $+0.08$ eV. This indicates that the core levels of the down atoms may overlap in energy with the bulk core levels although their bonding character is different. We find -0.56 and -0.28 eV for the second-adlayer atoms which are bonded to the up and down atoms of the top-adlayer Si atoms, respectively. The substrate-surface layer atoms show a core-level shift of -0.3 eV.

The discrepancy between our results and experiment may have one or more of the following reasons: (1) different procedures for fitting the experimental data may give rise to different results. In the raw data of the spectra (see Fig. 2 of Ref. 22), only the peak $S1$ is obvious but the other two peaks $S2$ and $S3$ are very weak, (2) the sample used in experiment may not have been perfect. The surface may be a mixture of regions reconstructed according to the most stable TAADM and to the metastable DDRM and SDRM, (3) our calculations of the core-level shifts may not be accurate enough, and (4) or our model does not correctly describe the surface investigated in the experiment. STM and core-level photoemission investigations of the very same sample may be necessary before one can convincingly assess the real (3×2) configuration.

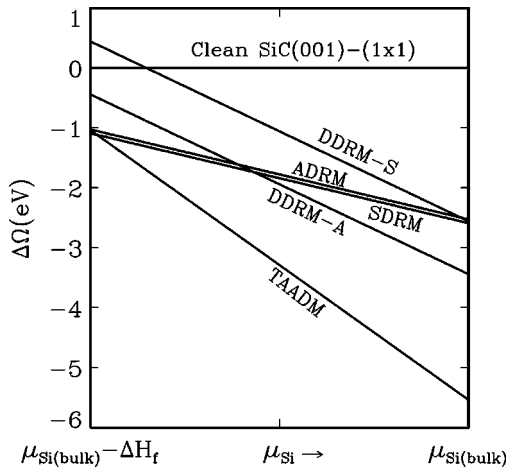

FIG. 10. Grand canonical potential per (3×2) unit cell for the different structures investigated in this work.

VI. GRAND CANONICAL POTENTIAL

The comparison of grand canonical potentials of structures with different stoichiometries or different adatom coverages is a very powerful means to arrive theoretically at optimal surface structures. As suggested by Qian, Martin, and Chadi,[35] as well as by Northrup and Froyen,[36] the difference of the grand canonical potentials of competing structures with different Si adatom coverages and that of the clean Si-terminated surface can be written as

$$\Delta\Omega = E - E_0 - \Delta n \cdot \mu_{Si},$$

where E and E_0 are the total energies of the considered reconstructed structure and the clean surface, respectively. Δn is the number of Si adatoms per unit cell and μ_{Si} is the chemical potential of atomic Si with an upper limit of $\mu_{Si(bulk)}$ and a lower limit of $\mu_{Si(bulk)} - \Delta H_f$. For the value of $\mu_{Si(bulk)}$, we use a computed value of -7.91 Ry in accordance with the employed pseudopotential. For the plot, we have used the measured heat of formation ΔH_f of bulk β-SiC of 0.72 eV.[37]

The grand canonical potentials for the different structures investigated in this work are shown in Fig. 10 as a function of the chemical potential μ_{Si}. Quite obviously, all structural models containing Si adatoms are more stable than the clean ideal SiC(001)-(1×1) surface for almost the complete allowed range of the chemical potential. Throughout the entire allowed range of μ_{Si}, the grand canonical potential of the TAADM with $\Theta=1$ is lowest in energy. This clearly indicates that the TAADM is the most stable model of all considered structures. In the case of $\Theta=2/3$, the symmetric-dimer structure is not favorable as compared to the asymmetric-dimer structures. Since the total energies of the four possible models for $\Theta=2/3$ are very close, we show them by one representative line labeled DDRM-A. In the upper limit of μ_{Si}, the DDRM's are more stable than the SDRM, while the opposite is true in the lower limit of μ_{Si}.

To shed some light on the question *why* the TAADM with $\Theta=1$ is the most stable structure, it is very revealing to count the number of dangling bonds in the different structures. In the TAADM, there are only two dangling bonds per (3×2) surface unit cell. One is localized at the up atom and

the other one at the down atom of the dimers in the top adlayer. All bonds from atoms in the second adlayer and in the substrate-surface layer are saturated by adatoms or by dimerization. In the SDRM, there are also two dangling bonds per surface unit cell localized at the adatoms. But in this case, the surface-layer atoms do not form real dimers with a correspondingly short dimer-bond length but they only move a little bit towards each other. In the DDRM's, there are four dangling bonds per unit cell localized at the top layer adatoms. Therefore these models are energetically less favorable than the TAADM.

In order to investigate the effect of an increase of the Si coverage beyond that of the TAADM we have also studied the case of $\Theta = 1.33$ ML. This structure turns out to be less stable than the (3×2) TAADM in the whole range of the allowed Si chemical potential. Therefore the (3×2) TAADM is the fully Si-saturated surface within the framework of our calculations. This is in agreement with the experimental observation.

VII. SUMMARY

We have investigated a number of Si-adatom induced (3×2) reconstructions of cubic SiC(001). Based on the results of our calculations, a model containing two Si adlayers with asymmetric dimers in the top adlayer, the TAADM, is suggested in order to explain the experimentally observed (3×2) reconstruction of this surface. The coverage of Si adatoms in our most stable model is $\Theta = 1$. Nevertheless, the structure does not simply consist of an adsorbed Si monolayer. Instead, two adlayers, each with a nominal coverage less than 1, are adsorbed on the clean Si-terminated SiC(001) surface. The first adsorbed adlayer, i.e., the top layer of the system, contains 1/3 of a Si monolayer and the second adsorbed layer contains 2/3 of a Si monolayer. In each (3×2) unit cell, there are two adatoms in the top layer and four adatoms in the second adlayer. All the bonds of Si atoms in the second adlayer and in the Si substrate-surface layer are saturated by adatoms or by dimerization. The dimer-bond lengths in the top adlayer, the second adlayer, and the substrate-surface layer are 2.21, 2.38, and 2.41 Å, respectively. There are only two dangling bonds per (3×2) unit cell localized at the atoms in the top adlayer. From the analysis of the grand canonical potential, we find that this structure is the most stable one in the entire allowed range of the chemical potential μ_{Si}. The calculated surface-band structure, as well as the filled D_b- and empty D_a-state STM images are in very good agreement with STM, as well as ARPES data.[8,9,28,29] The existence of the three types of defects observed in STM experiments[9] can be rationalized within this model. The adatom coverage $\Theta = 1$ is also compatible with RHEED data.[33]

In the case of $\Theta = 2/3$, the double-dimer-row models fail to be in accord with the measured surface-band structure and STM images observed in experiment. The strong interaction between the dimer rows results in a strong dispersion of the surface bands along the Γ-J line.

In the case of $\Theta = 1/3$, two models, the single-dimer-row and the alternate-dimer-row model are investigated. The ADRM can be excluded on the basis of LEED,[5] as well as other experimental data[3] and our total-energy results which also show that the ADRM is less favorable than the SDRM. The latter model fails to explain the measured STM images, especially the two spots per unit cell along the $3\times$ direction in the empty D_{down}-state STM image. Since the dimer in the SDRM is parallel to the $\times2$ direction, the empty-state STM image shows two spots along the $\times2$ direction.

In conclusion, our proposed two adlayer asymmetric-dimer model (TAADM) with $\Theta = 1$, is the most stable (3×2) reconstruction among all the structures which we have considered. This model is in very good accord with experimental ARPES and STM data. In addition, it can be successfully used to rationalize the occurrence of three types of surface defects, as well as the disorder features observed in empty-state STM images.

ACKNOWLEDGMENTS

We acknowledge financial support of this work by the Deutsche Forschungsgemeinschaft (Bonn, Germany) under Contract No. Po 215/13-1 and by a grant of Cray computer time at the Höchstleistungsrechenzentrum (HLRZ) of the Forschungszentrum Jülich (Germany) under Contract No. K2710000.

[1] V. M. Bermudez, Phys. Status Solidi B **202**, 447 (1997).
[2] J. Pollmann, P. Krüger, and M. Sabisch, Phys. Status Solidi B **202**, 421 (1997).
[3] M. Dayan, J. Vac. Sci. Technol. A **4**, 38 (1986).
[4] S. Hara, W. F. J. Slijkerman, J. F. van der Veen, I. Ohdomari, S. Misawa, E. Sakuma, and S. Yoshida, Surf. Sci. Lett. **231**, L196 (1990).
[5] R. Kaplan, Surf. Sci. **215**, 11 (1989).
[6] V. M. Bermudez and J. P. Long, Appl. Phys. Lett. **66**, 475 (1995).
[7] M. L. Shek, Surf. Sci. **349**, 317 (1996).
[8] S. Hara, J. Kitamura, H. Okushi, S. Misawa, Y. Yoshida, and Y. Tokumaru, Surf. Sci. **357-358**, 436 (1996).
[9] F. Semond, P. Soukiassian, A. Mayne, G. Dujardin, L. Douillard, and C. Jaussaud, Phys. Rev. Lett. **77**, 2013 (1996).
[10] P. Soukiassian, F. Semond, L. Douillard, A. Mayne, G. Dujardin, L. Pizzagalli, and C. Joachim, Phys. Rev. Lett. **78**, 907 (1997).
[11] V. Yu. Aristov, L. Douillard, O. Fauchoux, and P. Soukiassian, Phys. Rev. Lett. **79**, 3700 (1997).
[12] M. Sabisch, P. Krüger, A. Mazur, M. Rohlfing, and J. Pollmann, Phys. Rev. B **53**, 13 121 (1996).
[13] P. Käckell, J. Furthmüller, and F. Bechstedt, Appl. Surf. Sci. **104-105**, 45 (1996).
[14] H. Yan, A. P. Smith, and H. Jónsson, Surf. Sci. **330**, 265 (1995).
[15] A. Catellani, G. Galli, and F. Gygi, Phys. Rev. Lett. **77**, 5090 (1996).
[16] B. I. Craig and P. V. Smith, Surf. Sci. **233**, 255 (1990).
[17] A. Catellani, G. Galli, F. Gygi, and F. Pellacini, Phys. Rev. B **57**, 12 255 (1998).
[18] L. Douillard, F. Semond, V. Yu. Aristov, P. Soukiassian, B. Delley, A. Mayne, G. Dujardin, and E. Wimmer, Mater. Sci. Forum **379**, 264 (1999).

[19] W. Lu, P. Krüger, and J. Pollmann, Phys. Rev. Lett. **81**, 2292 (1998).
[20] M. Kitabatake and J. E. Greene, Appl. Phys. Lett. **69**, 2048 (1996); Jpn. J. Appl. Phys., Part 1 **35**, 5261 (1996).
[21] J. Tersoff, Phys. Rev. B **38**, 9902 (1988).
[22] H. W. Yeom, Y.-C. Chao, S. Terada, S. Hara, S. Yoshida, and R. I. G. Uhrberg, Phys. Rev. B **56**, R15 525 (1997).
[23] W. Kohn and L. J. Sham, Phys. Rev. **140**, A1133 (1965).
[24] L. Kleinman and D. M. Bylander, Phys. Rev. Lett. **48**, 1425 (1982).
[25] D. M. Ceperley and B. J. Alder, Phys. Rev. Lett. **45**, 566 (1980).
[26] J. P. Perdew and A. Zunger, Phys. Rev. B **23**, 5048 (1981).
[27] J. Tersoff and D. Hamann, Phys. Rev. B **31**, 805 (1985).
[28] K. Lindner, diploma thesis, Technical University Chemnitz, 1997.
[29] M. Lübbe, K. Lindner, S. Sloboshanin, S. Tautz, J. Schäfer, and D. R. T. Zahn, J. Vac. Sci. Technol. A **16**, 3471 (1998).
[30] H. W. Yeom, Y.-C. Chao, I. Matsuda, S. Hara, S. Yoshida, and R. I. G. Uhrberg, Phys. Rev. B **58**, 10 540 (1998).
[31] E. Pehlke and M. Scheffler, Phys. Rev. Lett. **71**, 2338 (1993).
[32] P. Krüger and J. Pollmann, Phys. Rev. Lett. **74**, 1155 (1995).
[33] T. Yoshinobu, I. Izumikawa, H. Mitsui, T. Fuyuki, and H. Matsunami, Appl. Phys. Lett. **59**, 2844 (1991).
[34] S. Hara, S. Misawa, S. Yoshida, and Y. Aoyagi, Phys. Rev. B **50**, 4548 (1994).
[35] G.-X. Qian, R. M. Martin, and D. J. Chadi, Phys. Rev. B **38**, 7649 (1988).
[36] J. E. Northrup and S. Froyen, Phys. Rev. Lett. **71**, 2276 (1993).
[37] O. Kubaschewski and C. B. Alcock, *Metallurgical Thermochemistry* (Pergamon, Oxford, 1979).